Photoionization of atoms and molecules studied by the Crank-Nicolson method

Xue-Bin Bian*

State Key Laboratory of Magnetic Resonance and Atomic and Molecular Physics, Wuhan Institute of Physics and Mathematics, Chinese Academy of Sciences, Wuhan 430071, People's Republic of China

(Received 29 July 2014; published 4 September 2014)

The Crank-Nicolson (C-N) method combined with a B-spline basis set can be used in both time-dependent and time-independent calculations of the photoionization cross sections of atoms and molecules. For time-independent systems, the imaginary-time propagation (ITP) method can usually only converge an arbitrary initial state to the ground state directly. Contrary to existing methods, it is found that the C-N method can converge an arbitrary initial state directly to not only the ground state but also excited and continuum states by controlling the time-step size. It is very useful if one is interested in only part of the spectral information since the computation is relatively cheap. The C-N method can also be directly applied in time-dependent calculations. During the time evolution, the spectral information, such as energy and momentum, can be retrieved by projecting the wave function on the eigenstates obtained using the ITP method. Both time-dependent and time-independent calculations agree very well with previous results. This method can also be extended to two-electron systems directly.

DOI: 10.1103/PhysRevA.90.033403 PACS number(s): 33.80.Rv, 31.15.−p

I. INTRODUCTION

Photoionization of atoms and molecules is a fundamental physical process which has been studied for many years. Proper and efficient accounting of high-lying excited states of the discrete and the continuous spectrum is necessary for the ionization dynamics of Rydberg states. Accurate solution of continuum states is an essential task in the various quantum-mechanical problems, such as the calculation of multiphoton ionization, above-threshold ionization (ATI), and electron scattering. However, the wave functions of continuum states oscillate to infinity. As a result, the calculations of the continuum states are not as easy as those of low-lying bound states using L^2 basis functions.

There are a number of methods to calculate the resonance states. The complex scaling method [1] rotates the coordinates into the complex plane, which allows us to solve the resonance states using the L^2 basis set. However, it is complex to apply it in time-dependent calculations. Although the variational method [2,3] and least-squares schemes [4] have been introduced in the calculation of continuum wave functions, efficient and accurate solutions are still necessary. In general, a variational approach can be used to calculate all the eigenstates of any quantum system using some appropriate basis set. After direct diagonalization of a Hamiltonian matrix for appropriate potentials, all the eigenvalues and wave functions are obtained. Negative eigenvalues correspond to bound states, while positive eigenvalues correspond to the continuum states. However, this method is not efficient for large-scale matrix problems involving large basis sets for convergence and high accuracy. In any standard matrix diagonalization program, the demand on computer memory grows as N^2, and the CPU time grows as N^3 (N is the size of the Hamiltonian matrix) [5]. When $N > 10\,000$, the computation becomes very slow, even impractical in some cases. It becomes much more complicated when arbitrary electronic structures and multichannel continua are involved. In addition, the obtained discrete continuum states may not be what we want because we do not know their boundary conditions. It is very expensive to obtain all the spectral information for a large Hamiltonian matrix.

However, the imaginary-time-propagation (ITP) method is quite efficient if only part of the eigenstates is needed. For certain chemical and physical problems, not all the eigenstates of a system are required. For example, to numerically solve time-dependent Schrödinger equations (TDSE), one only needs the initial wave function and then propagates it under a Hamiltonian including time-dependent interaction terms by using general split-operator methods (SOM) [6,7] or efficient large-vector-matrix operations [8,9]. If the initial state in a simulation is the ground state, one does not need to diagonalize a basis-set-dependent Hamiltonian, but one propagates a TDSE for an arbitrary initial vector using the ITP method [10]. The above existing methods can only converge an arbitrary state to the ground state directly. In this paper, we show that ITP method based on the Crank-Nicolson (C-N) [11,12] scheme can be generalized to converge to bound exited and unbound continuum states directly by changing the time step. To our knowledge, this has not been reported. The ITP calculations and time-dependent calculations based on the C-N method agree very well.

This paper is organized as follows: The principle of the ITP method for excited and continuum states is presented in Sec. II. The application of the ITP method in the photoionization of one-electron diatomic molecular ions H_2^+ and HeH^{2+} is shown in Sec. III. In Sec. IV, we illustrate the application of the proposed ITP method in two-electron systems. The paper concludes in Sec. V.

II. PRINCIPLE OF THE ITP METHOD

In this section, we briefly introduce the principle of the usual ITP method for the ground state and our proposed ITP method based on the C-N scheme for all the bound and continuum states.

*xuebin.bian@wipm.ac.cn

A. Usual ITP method for the ground state

The principle of the ITP method can be found as follows. For a general TDSE (atomic units, $e = \hbar = m_e = 1$, are used unless otherwise specified),

$$i\frac{\partial}{\partial t}|\Psi(\mathbf{r},t)\rangle = H|\Psi(\mathbf{r},t)\rangle, \tag{1}$$

introducing the imaginary time $t \to -it$ in an ITP method, and if the Hamiltonian H is time independent, then the new time-dependent wave function after a time step Δt can be written as

$$|\Psi(\mathbf{r},\Delta t)\rangle = \exp^{-H\Delta t}|\Psi(\mathbf{r},0)\rangle. \tag{2}$$

Expanding an initial arbitrary wave function $|\Psi(\mathbf{r},0)\rangle$ as a linear combination of the time-independent eigenstates $\varphi_n(\mathbf{r})$ of H,

$$|\Psi(\mathbf{r},0)\rangle = \sum_n a_n\varphi_n(\mathbf{r}), \tag{3}$$

where $H\varphi_n(\mathbf{r}) = E_n\varphi_n(\mathbf{r})$, Eq. (2) can be written as

$$|\Psi(\mathbf{r},\Delta t)\rangle = \sum_n \exp^{-E_n\Delta t} a_n\varphi_n(\mathbf{r}). \tag{4}$$

It is obvious that higher-energy states will exponentially decay as a function of $E\Delta t$ [see Fig. 1(a)] at a rate which is faster than that for the lower-energy states. After a sufficiently long time evolution, any arbitrary initial wave function will thus converge to the ground state. If we are interested in an excited state $\varphi_n(\mathbf{r})$, we have to first obtain the converged ground state $\varphi_1(\mathbf{r})$ and other lower excited states $\varphi_{n'}(\mathbf{r})$, with $n' = 2,3,\ldots,n-1$, then project out all the lower-energy states by $(1 - \sum_{n'=1}^{n-1}|\varphi_{n'}(\mathbf{r})\rangle\langle\varphi_{n'}(\mathbf{r})|)$ from the initial state before evolution [13]. For higher excited states, this method becomes slowly convergent and difficult to apply. It is not even practical for continuum states due to the large degeneracy of those states.

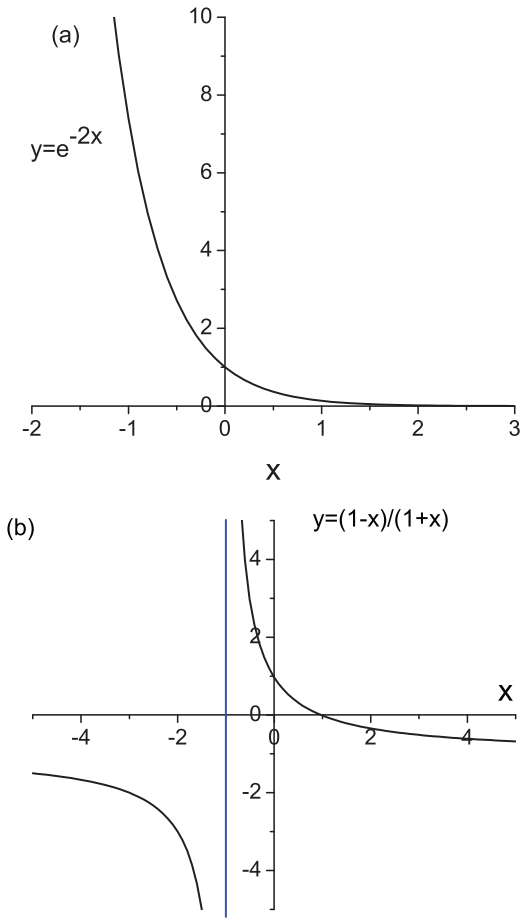

FIG. 1. (Color online) Prefactors of Eqs. (4) and (6) as a function of $x = E\Delta t/2$.

B. C-N ITP method for any bound state

We show next that by using the C-N and ITP methods, we can simply restrict any initial arbitrary state to converge to desired excited states by changing the appropriate time step Δt of the iteration. It can also be easily extended to calculate any continuum state, such as the final states in photoionization. The principle of the C-N ITP method is similar to inverse iteration.

The C-N method is a unitary and unconditionally stable method [11,12]. It is based on expressing the exponential operator $\exp^{-H\Delta t}$ to second-order accuracy in Eq. (2) as

$$\exp^{-H\Delta t} = \frac{1 - H\Delta t/2}{1 + H\Delta t/2} + O(\Delta t^3). \tag{5}$$

Then Eq. (4) can be equivalently written for any arbitrary state,

$$|\Psi(\mathbf{r},\Delta t)\rangle = \sum_n \frac{1 - E_n\Delta t/2}{1 + E_n\Delta t/2} a_n\varphi_n(\mathbf{r}). \tag{6}$$

Setting $x = E_n\Delta t/2$, the factor in Eq. (6) is $\frac{1-x}{1+x} = 1 - \frac{2}{1+\frac{1}{x}}$, which does not evolve with exponential decay but has a maximum around $x = -1$, as shown in Fig. 1(b). As a result, after long-time evolution, only the eigenstate with $E_n\Delta t/2 \approx -1$ remains dominant in the superposition of states in Eq. (6). However, in practice, since nondegenerate bound-state energies are separated, $E_n\Delta t/2 \approx -1$ is not a strict condition. We do not need to project out other lower bound states as described in Sec. II A. As long as the absolute "action" distance $|E_n\Delta t/2 + 1|$ is smaller than that of other bound states, the state with energy E_n will remain while other states decay faster. Choosing a time step Δt which is positive and small enough, with $E_1\Delta t/2 > -1$ or $\Delta t < 2/|E_1|$, Eq. (6) will converge to the ground state with the lowest eigenvalue E_1. If one then gradually increases the time step Δt, when $E_2\Delta t/2 + 1 < -1 - E_1\Delta t/2$, the ground state and other excited states excluding the first excited state will decay, thus converging to the first excited state. Similarly, by further iteration, we can obtain other converged excited states directly only by gradually increasing the time step Δt; that is, the process filters out all undesired states except one.

As a demonstration of the proposed method, we calculate the s bound states of H. The wave function is expanded in radial B splines [14–16] and angular spherical harmonics as

$$|\Psi(\mathbf{r},t)\rangle = \sum_{i=1}^{N} C_i(t)\frac{B_i^k(r)}{r}Y_l^m(\theta,\varphi), \tag{7}$$

where $l = m = 0$, $C_i(t)$ is the time-dependent coefficients of the corresponding B splines, and k is the order of the B splines.

TABLE I. Comparison of the eigenvalues of H s states obtained using the ITP method with time step Δt and iterations j and the analytic values $-1/2n^2$ (a.u.). $\Delta t = 2,10$, and 40 a.u. for E_1, E_2, and E_3, respectively.

j	E_1 (a.u.)	E_2 (a.u.)	E_3 (a.u.)
1	0.02074985099579411	0.01704393876353220	−0.03172899941642318
2	−0.004.535732379123197	−0.02707373759307351	−0.05502525262084053
3	−0.157925711875305	−0.102192312548041	−0.05553857185259704
4	−0.440683975870317	−0.122870665895126	−0.05555477488356365
5	−0.494240272539091	−0.124820611212683	−0.05555551614437183
6	−0.499235363892429	−0.124985275640302	−0.05555555352112400
7	−0.499870405769063	−0.124999310529914	−0.05555555544994874
8	−0.499975900374919	−0.125000203414494	−0.05555555555006548
9	−0.499995389821222	−0.125000111564971	−0.05555555555526998
10	−0.499999110747678	−0.125000039965192	−0.05555555555554072
11	−0.499999828045146	−0.125000012764312	−0.05555555555555482
12	−0.499999966722960	−0.125000003889258	−0.05555555555555550
13	−0.499999993558485	−0.125000001158381	−0.05555555555555556
14	−0.499999998752989	−0.125000000340924	−0.05555555555555559
15	−0.499999999758584	−0.125000000099687	−0.05555555555555550
16	−0.499999999953262	−0.125000000029042	−0.05555555555555559
17	−0.499999999990952	−0.125000000008444	−0.05555555555555552
18	−0.499999999998248	−0.125000000002452	−0.05555555555555557
19	−0.499999999999661	−0.125000000000712	−0.05555555555555549
20	−0.499999999999934	−0.125000000000207	−0.05555555555555556
21	−0.499999999999987	−0.125000000000060	−0.05555555555555559
22	−0.499999999999997	−0.125000000000017	−0.05555555555555559
23	−0.499999999999999	−0.125000000000005	−0.05555555555555555
24	−0.499999999999999	−0.125000000000002	−0.05555555555555554
25	−0.500000000000000	−0.125000000000000	−0.05555555555555555
$-1/2n^2$	−0.5	−0.125	−0.0555555555555555(5)

The corresponding Hamiltonian is written as

$$H = -\frac{1}{2}\frac{d^2}{dr^2} + \frac{l(l+1)}{2r^2} - \frac{1}{r}. \tag{8}$$

The time evolution at each step Δt of the coefficients in Eq. (7) in the C-N method can be written as

$$(\mathbf{S} + \mathbf{H}\Delta t/2)\mathbf{C}(\Delta t) = (\mathbf{S} - \mathbf{H}\Delta t/2)\mathbf{C}(0), \tag{9}$$

where $\mathbf{S}$ and $\mathbf{H}$ are the overlap and Hamiltonian matrix [5,16], respectively, for Eq. (8) in the B-spline basis. Since B splines are a localized basis [14], $\mathbf{S}$ and $\mathbf{H}$ are sparse band matrices, which greatly reduces the memory and computation time. In practical calculations, the right side of Eq. (9) is a matrix vector multiplication. Then $\mathbf{C}(\Delta t)$ can be obtained by solving sparse linear equations.

In our calculation, the radial space dimension is truncated at $r_{\max} = 100$ a.u.; the wave function is expanded by $N = 200$ B splines with order $k = 7$. The convergence speed depends on the guess of the initial state. To show the generality of the ITP method, the initial coefficients are set as $C_i(0) = 1/\sqrt{N}$ for $i = 1,2,\ldots,N$. As illustrated in Table I, with a time step $\Delta t = 2$ a.u., which satisfies $\Delta t < 2/|E_1|$, convergence to the ground state is obtained readily with energy $E_1 = -0.5$ a.u. with machine accuracy after 25 iterations. When we increase the time step to $\Delta t = 10$ a.u., which satisfies the condition $E_2\Delta t/2 + 1 < -1 - E_1\Delta t/2$ as discussed above, the first excited state $n = 2$ is obtained. Similarly, other higher excited states can be easily obtained directly by controlling the time step Δt. The required iteration number j is not sensitive to the matrix order N. We have tested the case with $N = 100\,000$, and $j = 40$ is large enough to converge the initial state to the desired eigenstate with machine precision. This method is not restricted to previous known systems, but it is a general method, as shown next.

C. C-N ITP method for continuum states

For field-free continuum states with positive energy E_c, except for the direct diagonalization [14], there is a least-squares method [17,18] to obtain E_c and Ψ_c. This is based on the idea of minimizing the residual vector $(H - E)\Psi$. We show next that we can directly extend the ITP method to obtain any continuum state. As shown above, the ITP method converges an arbitrary vector to the bound eigenstate φ_n at the action value $E_n\Delta t/2 \approx -1$ or energy $E_n \approx -2/\Delta t$. If we want the continuum states with $E_c > 0$, we only have to change the sign of the time step $\Delta t \to -\Delta t$ in the above restriction; equivalently, we transform the TDSE in Eq. (1) using a new ITP method with $t \to it$. Then the arbitrary initial state converges to continuum state Ψ_c with positive energy $E_c \approx 2/\Delta t$. For bound states, we do not know the energies and wave functions, but the boundary condition $\varphi_n(r_{\max}) = 0$ is known. However, for a continuum state, its energy is known, we do not know the boundary condition, and the above process will not exactly converge to E_c. Since the wave functions of continuum states oscillate to infinity, there must be a series of points r_c with $\Psi_c(r_c) = 0$ [19,20]. In practice, we can safely set the initial boundary condition $\Psi_c(r_{\max}) = 0$ in our calculations. Then

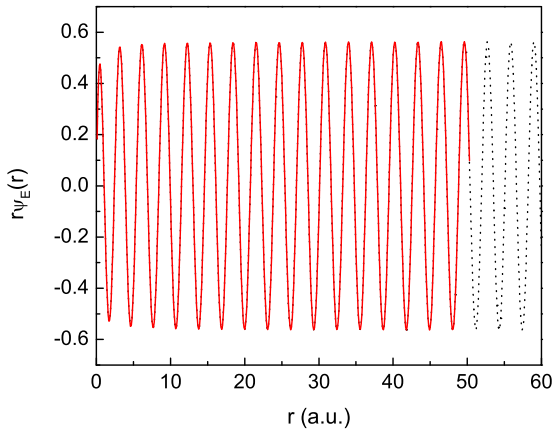

FIG. 2. (Color online) Comparison of hydrogen continuum radial state $r\Psi_E(r)$ obtained using the ITP method (with iterations $j = 18$; solid line) with the analytic Coulomb wave function (dotted line) with $l = 0$, $E = 2$ a.u. Both are normalized on the energy scale.

Δt is set to be $2/E_c$, and the energy E is obtained by ITP. Usually, E is linearly dependent on $r_{\max}$. If the converged E is not equal to E_c, we smoothly change the size of the box $r_{\max}$ in the ITP method until the expected eigenvalue $\langle\Psi|H|\Psi\rangle/\langle\Psi|\Psi\rangle$ matches the desired eigenvalue E_c with required accuracy [14], then we can say $r_{\max} = r_c$. To calculate the continuum state with energy $E_c = 2$ a.u., we propagate an arbitrary vector with a time step $\Delta t = 1$ a.u. The wave function obtained after $j = 18$ iterations is illustrated in Fig. 2, which is normalized on the energy scale. We also plot the exact regular Coulomb wave function as a comparison in Fig. 2. The illustrated result clearly shows that this new ITP method for obtaining continuum states is very accurate.

III. APPLICATIONS OF THE ITP METHOD IN PHOTOIONIZATION OF ONE-ELECTRON DIATOMIC MOLECULES

Molecular systems are more complex than atoms. There are no simple exact analytic solutions even for the simplest one-electron molecular ion $H_2{}^+$ [21,22]. Although a Green's function in spheroidal coordinates can be obtained with the quantum defect method [23,24], accurate numerical solutions are very useful, especially for the TDSE [18]. In this section we will show that our ITP method can be directly extended to diatomic molecular systems.

We use prolate spheroidal coordinates (ξ,η,ϕ) to represent the electron. ϕ is the azimuthal angle, and the internuclear distance is R. If r_1 and r_2 are the distances of the electron from the two nuclei, we have

$$\xi = (r_1 + r_2)/R, \quad \eta = (r_1 - r_2)/R, \tag{10}$$

with $\xi \in [1,\infty]$, $\eta \in [-1,1]$. The field-free Hamiltonian in the fixed-nuclei approximation is [15]

$$H_0 = -\frac{1}{2}\nabla^2 + V$$
$$= -\frac{2}{R^2(\xi^2-\eta^2)}\left[\frac{\partial}{\partial\xi}\left((\xi^2-1)\frac{\partial}{\partial\xi}\right)\right.$$
$$\left. + \frac{\partial}{\partial\eta}\left((1-\eta^2)\frac{\partial}{\partial\eta}\right) + \left(\frac{1}{\xi^2-1} + \frac{1}{1-\eta^2}\right)\frac{\partial^2}{\partial\phi^2}\right]$$
$$-2\frac{(Z_1+Z_2)\xi - (Z_1-Z_2)\eta}{R(\xi^2-\eta^2)}, \tag{11}$$

where Z_1 and Z_2 are the nuclear charges. We expand the electronic wave function in a B-spline basis [15] as follows:

$$\psi(\xi,\eta,\varphi) = \sum_{i,j,m} C^m_{i,j}(\xi^2-1)^{\frac{|m|}{2}} B_i(\xi)(1-\eta^2)^{\frac{|m|}{2}} B_j(\eta)\frac{e^{im\phi}}{\sqrt{2\pi}}.$$

The volume element is $d\tau = (R/2)^3(\xi^2-\eta^2)d\xi d\eta d\phi$. For $H_2{}^+$, $Z_1 = Z_2 = 1$. We have calculated the bound-state energy with $m = 0$, $R = 2$ a.u. The η dimension is expanded into 20 B splines with order 7. The ξ direction is truncated at $\xi_{\max} = 80$ a.u. and is expanded by 80 B splines with order 7. The results with iterations $j = 8$ are presented in Table II as a comparison with Ref. [22]. Our present method with a small number of iterations j or total time $t = j\Delta t$ is very accurate with a small basis and converges faster to the desired states than usual methods.

TABLE II. Comparison of the $m = 0$ eigenvalues of $H_2{}^+$ obtained with the ITP method and the values in Ref. [22]. The internuclear distance is $R = 2$ a.u.; the iterations $j = 8$ in the ITP method.

State	Δt (a.u.)	E in ITP (a.u.)	E in Ref. [22] (a.u.)
$1\sigma_g$	2	−1.1026342144949	−1.1026342144949
$1\sigma_u$	3	−0.6675343922023	−0.6675343922024
$2\sigma_g$	6	−0.3608648753394	−0.3608648753383
$2\sigma_u$	8	−0.2554131650864	−0.2554131650857

The two-center wave function is also separable as

$$\psi(\xi,\eta,\phi) = U(\xi)V(\eta)\Phi(\phi), \tag{12}$$

where $\Phi(\phi) = \frac{e^{im\phi}}{\sqrt{2\pi}}$ and $U(\xi)$ and $V(\eta)$ satisfy separate differential equations,

$$\frac{d}{d\xi}\left[(\xi^2-1)\frac{dU}{d\xi}\right] + \left[-A_{mq} + c^2(\xi^2-1) + a\xi - \frac{m^2}{\xi^2-1}\right]U = 0, \tag{13}$$

$$\frac{d}{d\eta}\left[(1-\eta^2)\frac{dV}{d\eta}\right] + \left[A_{mq} + c^2(1-\eta^2) + b\eta - \frac{m^2}{1-\eta^2}\right]V = 0, \tag{14}$$

where A_{mq} is the separation constant, $a = R(Z_1+Z_2)$, $b = R(Z_2-Z_1)$, $c^2 = R^2E/2$.

For a continuum state with energy E_c, A_{mq} [where q is equal to the number of zeros of the function $V(\eta)$] can be calculated by expanding $V(\eta)$ in a series of associated Legendre polynomials [25]. It can also be obtained by a diagonalization of Eq. (14) [26] or using the ITP method introduced above. In the present work, we expand $V(\eta)$ into 20 B splines with order 7 and use the diagonalization method to have the separation constant A_{mq} and the corresponding

TABLE III. One-photon partial absorption cross sections [for comparison, Eq. (16) is divided by 3] from the H_2^+ ground state $1\sigma_g$ ($q = 0$). The internuclear distance is $R = 2$ a.u.; 1 Mb = 10^{-18} cm^2.

Photoelectron energy E_c (a.u.)	$p\sigma_u$ ($q = 1$) ($\times 10^{-2}$ Mb)	$f\sigma_u$ ($q = 3$) ($\times 10^{-2}$ Mb)
1	0.688[a]	0.907[a]
	0.694[b]	0.904[b]
	0.54[c]	0.94[c]
2	0.517[a]	0.618[a]
	0.516[b]	0.618[b]
4	0.202[a]	0.220[a]
	0.200[b]	0.222[b]
10	0.0140[a]	0.00192[a]
	0.0138[b]	0.00190[b]

[a]Present work.
[b]Reference [30].
[c]Reference [21].

$V(\eta)$. To calculate the radial wave function $U(\xi)$ in Eq. (13), we use the ITP method introduced above. Instead of fitting E_c, we smoothly vary the box $\xi_{\max}$ to fit the separation constant A_{mq} obtained from Eq. (14). The normalization of the radial function is realized by fitting the asymptotic behavior of $U(\xi)$ at $\xi \gg 1$ [27–29]:

$$U(\xi) \to \frac{1}{R\xi}\sqrt{\frac{8}{k\pi}}\sin\left(\frac{kR\xi}{2} + \frac{2}{k}\ln(kR\xi) - \frac{l\pi}{2} + \Delta\right), \tag{15}$$

where Δ is the phase of the radial function.

Once we have the continuum state, in examples discussed in the Introduction, one can calculate the general one-photon absorption partial cross sections given by [26]

$$\sigma_q = 4\pi^2\alpha\omega|\langle i|D|f\rangle|^2, \tag{16}$$

where $|i\rangle$ and $|f\rangle$ are the initial and final states, respectively. D is the transition operator z, which is $R\xi\eta/2$ in the length gauge. α is the fine-structure constant, and ω is the photon energy.

Table III shows the one-photon partial absorption cross sections from the H_2^+ ground state at equilibrium internuclear distance $R = 2$ a.u. to different continuum states $|f\rangle = |E_c\rangle$, where $E_c = h\nu - I_p$. Again, using the ITP method, our results agree well with those of Ref. [30] from low to very high energy. The relative difference is less than 1%. For the laser field polarization parallel to the molecular axis, we present the total one-photon ionization cross section σ_{total} as a function of photoelectron energy E_c in Fig. 3. It agrees well with the results from the complex scaling method [1]. The total cross sections have a maximum around $E_c = 0.8$ a.u. We also present the relative contribution of each partial wave to the total cross section in Fig. 4. Because of the symmetry, only the transitions to states with different parities are allowed. For lower photoelectron energy, the transition to $q = 3$ states is dominant. The contributions from $q = 1$ and $q = 3$ states are comparable in the high-energy region. The contribution of $q = 5$ states is almost negligible.

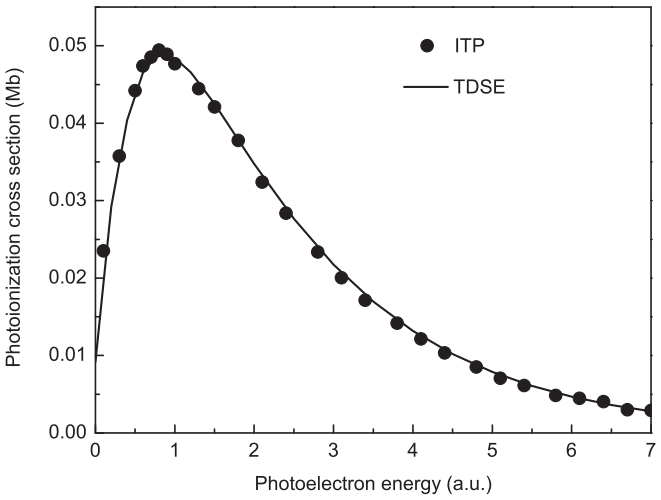

FIG. 3. One-photon ionization cross sections for H_2^+ as a function of photoelectron energy. The initial state is the ground $1\sigma_g$ state. The laser polarization is parallel to the molecular axis. The internuclear distance $R = 2$ a.u. The time-dependent results (solid line) are compared with those using the ITP method (circles).

The C-N method can also be used in real-time TDSE. For a very short time step Δt, Eq. (9) can be written as

$$\mathbf{C}(t + \Delta t) = \frac{\mathbf{S} - i\mathbf{H}(t + \Delta t/2)\Delta t/2}{\mathbf{S} + i\mathbf{H}(t + \Delta t/2)\Delta t/2}\mathbf{C}(t). \tag{17}$$

A sine-squared laser pulse with a duration τ of ten optical cycles with different photon frequencies is used in the calculation of TDSE. The intensity is $I = 1 \times 10^{13}$ W/cm^2. At the end of the pulse t_f, the one-photon ionization cross section is given by [31]

$$\sigma_{\text{total}} = \left(\frac{\omega}{I}\right)\frac{P}{T_{\text{eff}}}, \tag{18}$$

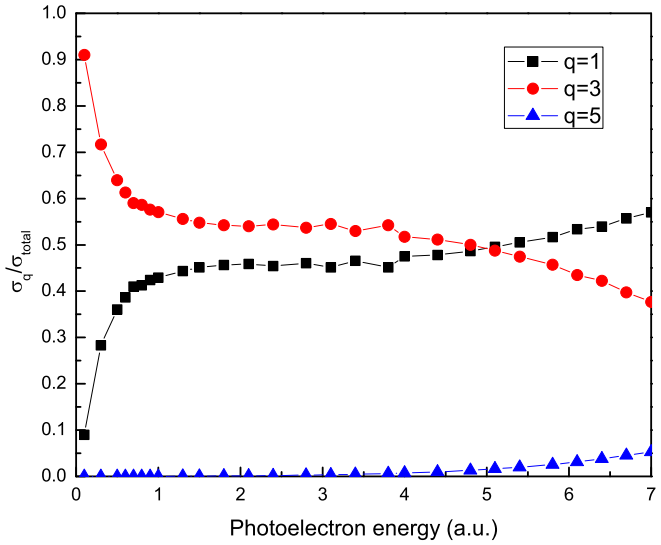

FIG. 4. (Color online) Relative contribution of each partial cross section σ_q to the total one-photon ionization cross section σ_{total}. The initial state is the ground $1\sigma_g$ state.

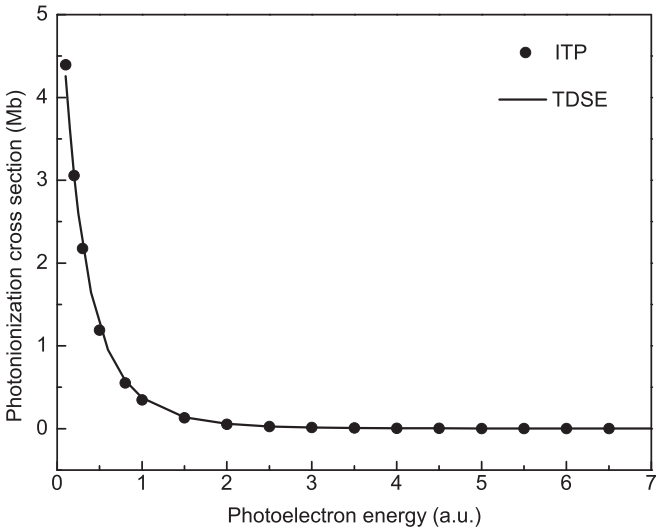

FIG. 5. Same as Fig. 3, but the initial state is the first excited state $1\sigma_u$.

where $T_{\rm eff} = \frac{3}{8}\tau$ and $P = 1 - \sum_n |\langle\varphi_n|\Psi(t_f)\rangle|^2$. The TDSE results are also presented in Fig. 3. One can see that the total one-photon ionization cross sections from the ITP method agree well those from TDSE.

We also calculated the one-photon ionization cross sections from the first excited state $1\sigma_u$ ($q = 1$) of $H_2{}^+$. The results of the ITP and TDSE methods are shown in Fig. 5. They also agree well with each other, showing the accuracy of our numerical methods. The total cross sections are significantly larger than those from the ground state due to its lower ionization potential, but they decay faster as the photoelectron energy increases. The contributions of each partial wave are illustrated in Fig. 6. As the photoelectron energy increases, the contribution from $q = 0$ states has a maximum around $E_c = 3$ a.u.; the contribution from $q = 2$ states has a fast decay

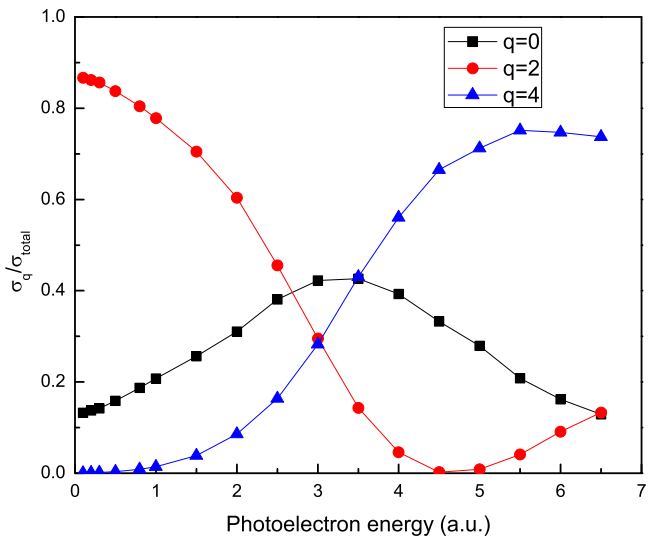

FIG. 6. (Color online) Same as Fig. 4, but the initial state is the first excited state $1\sigma_u$.

TABLE IV. Comparison of the $m = 0$ eigenvalues of HeH^{2+} obtained with the ITP method and the values in Ref. [35]. The internuclear distance is $R = 4$ a.u.; the iterations $j = 8$ in the ITP method.

State	Δt (a.u.)	E in ITP (a.u.)	E in Ref. [35] (a.u.)
$1s\sigma$	1	−2.250605387820	−2.250605387827
$2p\sigma$	2	−1.031081311774	−1.031081311774
$2s\sigma$	3	−0.6809853203162	−0.680985320316
$3p\sigma$	4	−0.4493213894454	−0.449321389445

with $E_c < 4.5$ a.u., then increases, while the contribution from $q = 4$ states gradually increases.

For the simplest asymmetric one-electron molecular ion HeH^{2+}, a number of features different from those of $H_2{}^+$ have been demonstrated in high-order-harmonic generation [15,32] and enhanced ionization (EI) [33,34]. We show next the application of the ITP method in the HeH^{2+} nonsymmetric system.

We fix the internuclear distance $R = 4$ a.u. (the equilibrium internuclear distance is around $R = 3.89$ a.u.). The eigenvalues of lower bound states obtained with the ITP method are presented in Table IV. They agree well with recent work [35]. The one-photon ionization cross sections from the ground $1s\sigma$ state of HeH^{2+} as a function of photoelectron energy with the ITP and TDSE methods are illustrated in Fig. 7. They agree very well and demonstrate a fast decay as a function of photoelectron energy. Due to the loss of symmetry, the final states may contain any partial wave. We expand the final wave with $q_{\rm max} = 6$ in the ITP method. The contribution of each partial wave is presented in Fig. 8. For $q = 0$, the contribution decays fast with the increase of photoelectron energy. The contributions of the $q = 1$ and $q = 4$ states have a maximum around $E_c = 1.5$ a.u., while the contributions of $q = 2$ and $q = 5$ states have a maximum around $E_c = 4$ a.u.

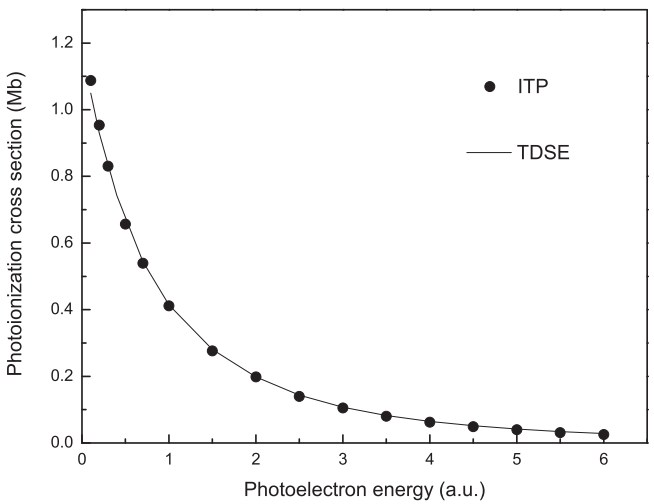

FIG. 7. One-photon ionization cross sections for HeH^{2+} as a function of photoelectron energy. The initial state is the ground $1s\sigma$ state. The laser polarization is parallel to the molecular axis. The internuclear distance $R = 4$ a.u. The time-dependent results (solid line) are compared with those from the ITP method (circles).

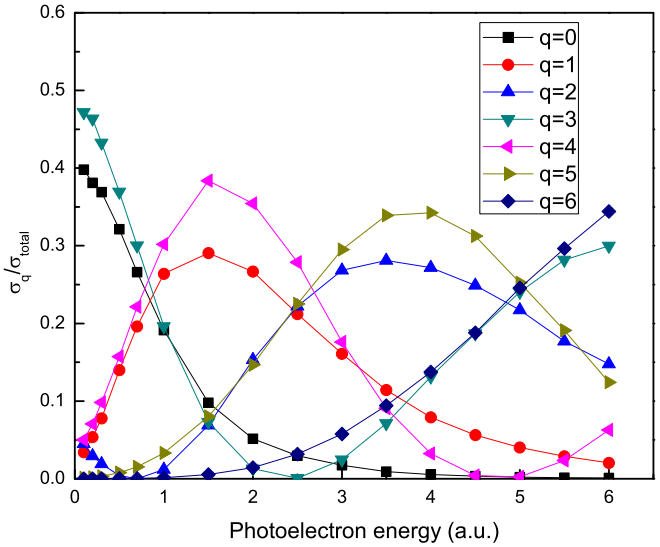

FIG. 8. (Color online) Relative contribution of each partial cross section σ_q to the total one-photon ionization cross section σ_{total}. The initial state is the ground $1s\sigma$ state.

The contribution of the $q = 3$ state has a minimum around $E_c = 2.5$ a.u. The contribution of the $q = 6$ state gradually increases as a function of photoelectron energy. Although the relative contribution of each partial wave is complex, the ITP method allows us to extract the information of each partial wave directly, which is important to calculate the angular distribution of photoelectrons [18,27].

The one-photon ionization cross sections from the first excited state $2p\sigma$ of HeH^{2+} as a function of photoelectron energy using the ITP and TDSE methods are illustrated in Fig. 9. They are similar to those of the $1s\sigma$ state, presenting a fast decay with the increase of photoelectron energy. The relative contribution of each partial wave shown in Fig. 10 is more complex than that in Fig. 8. The main contributions are from the $q = 2,3,4,6$ states.

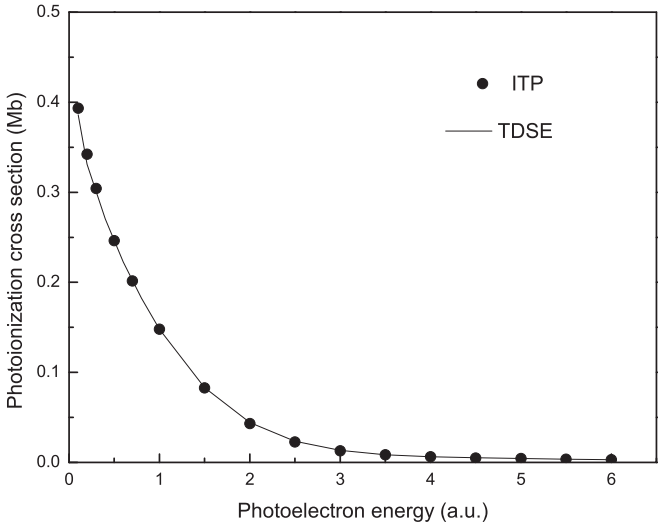

FIG. 9. Same as Fig. 7, but the initial state is the first excited state $2p\sigma$.

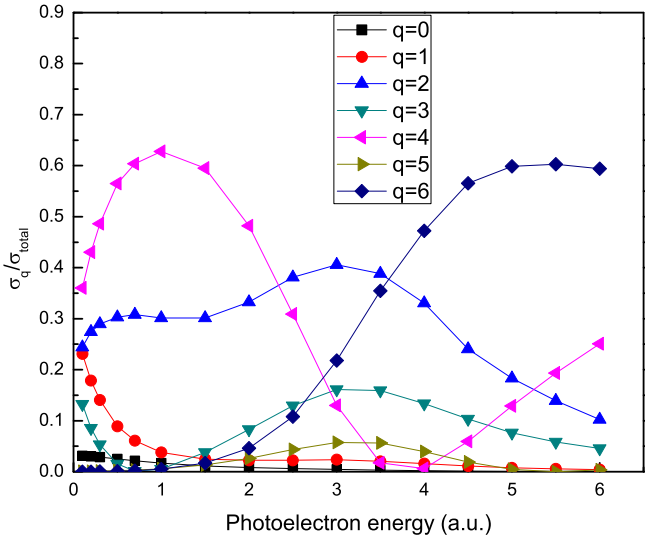

FIG. 10. (Color online) Same as Fig. 8, but the initial state is the first excited state $2p\sigma$.

IV. APPLICATIONS OF THE ITP METHOD IN TWO-ELECTRON SYSTEMS

It is very important to accurately solve the many-electron systems to study the electronic correlation effects. In this section, we extend our method to two-electron atomic systems [36,37]. The nonrelative Hamiltonian in Eq. (1) can be written as

$$H = \sum_{i=1}^{2}\left(\frac{\hat{\mathbf{p}}_i^2}{2} - \frac{Z}{r_i}\right) + \frac{1}{|\mathbf{r}_1 - \mathbf{r}_2|}, \tag{19}$$

where Z is the nuclear charge. The total electronic wave function is expanded in coupled spherical harmonics:

$$|\Psi(\mathbf{r}_1,\mathbf{r}_2,t)\rangle = \sum_{L,M}\sum_{l_1,l_2}\frac{\psi_{l_1l_2}^{LM}(r_1,r_2,t)}{r_1 r_2}\sum_{m_1,m_2} C_{m_1m_2M}^{l_1l_2L} Y_{m_1}^{l_1}(\Omega_1) Y_{m_2}^{l_2}(\Omega_2), \tag{20}$$

where $C_{m_1m_2M}^{l_1l_2L}$ is a Clebsch-Gordan coefficient and $\psi_{l_1l_2}^{LM}(r_1,r_2,t)$ is expanded by B splines as

$$\psi_{l_1l_2}^{LM}(r_1,r_2,t) = \sum_{i,j} C_{i,j}^{l_1,l_2,LM}(t) B_i(r_1) B_j(r_2). \tag{21}$$

The Hamiltonian matrix can be obtained easily except for the two-electron integrals. We expand the interelectron repulsion term by a multipole expansion:

$$\frac{1}{|\mathbf{r}_1 - \mathbf{r}_2|} = \sum_l \frac{(r_1,r_2)_<^l}{(r_1,r_2)_>^{l+1}} P_l(\cos\theta_{12}), \tag{22}$$

where $P_l(\cos\theta_{12})$ is a Legendre function. The angular integral can be done analytically, which is shown in Ref. [38]. The radial integral is based on Poisson's equation, which is introduced in Ref. [39]. Using the ITP method presented above, we calculated the S states of He. The radial space is truncated at $r_{\max} = 40$ a.u., and the radial wave function

TABLE V. Comparison of the eigenvalues of He S states obtained with the ITP method (the first entry) and the values in Ref. [37] (the second entry).

State	Singlet (a.u.)	Triplet (a.u.)
$1S$	-2.90370	
	-2.90372	
$2S$	-2.145972	-2.17522935
	-2.145974	-2.17522937
$3S$	-2.0612712	-2.06868904
	-2.0612719	-2.06868906
$4S$	-2.03356	-2.03650
	-2.03358	-2.03651

in Eq. (21) is expanded by 60 B splines with order 8. The angular part in Eq. (20) is expanded by $l_{1,\max} = l_{2,\max} = 10$. The two-electron integral in Eq. (22) is truncated with $l_{\max} = 35$. The obtained singlet and triplet eigenenergies are presented in Table V with a comparison of the values in Ref. [37]. In spite of small size of the basis, the accuracy of the obtained eigenvalues is up to five digits. The eigenvalue of the negative ion H^- is calculated in a very similar way by setting the nuclear charge $Z = 1$ in Eq. (19). It is known that there is only one bound state in H^- [40]. Our calculated energy $E = -0.52774$ a.u. agrees well with the accurate energy $E = -0.52775$ a.u. The results demonstrate that our method can be directly used in calculating bound states of three-body systems. However, the calculations of the correlated two-electron continuum states are still challenging.

V. CONCLUSION

In summary, the usual ITP methods can only converge an arbitrary initial state directly to the ground state. To obtain an excited state, they require filtering out all lower bound states from the initial state, which is inefficient and impractical in some cases. Based on the Crank-Nicolson numerical method, we present in this work an extension of the ITP method $t \to -it$ for directly converging an arbitrary initial vector to desired bound excited states by controlling the time step size. It greatly improves the efficiency of ITP for high-lying excited states, especially for Rydberg states. The usual ITP methods cannot converge to the continuum states with positive energies. In this work, we generalize the ITP method by $t \to it$ and show convergence of any arbitrary state to desired continuum states. This method is proven to be simple and accurate for a small number of iterations j or total time $t = j\Delta t$. The application of this ITP method to the photoionization of diatomic molecules is illustrated. This method can also be used in two-electron systems. We emphasize that this C-N method is a systematic method to study ultrafast dynamics. After obtaining the initial bound state by C-N ITP, the C-N method can be used to solve TDSE in real-time space. During the interactions between intense ultrashort laser pulses and atoms and molecules, the energy and momentum information of the photoelectrons can be extracted from the time-dependent wave functions [18] by projecting on the continuum states obtained by ITP. This method does not depend on the expression of the Hamiltonian explicitly, which can be directly extended to complex system [3], confined systems [41], Dirac equations [42], multiparticle states [36], and also time-dependent density-functional-theory methods [43,44] for complex molecular systems.

ACKNOWLEDGMENTS

The author thanks Prof. A. D. Bandrauk very much for helpful discussions. This work is supported by the National Natural Science Foundation of China under Grant No. 11404376.

[1] L. Tao, C. W. McCurdy, and T. N. Rescigno, Phys. Rev. A **79**, 012719 (2009).
[2] M. Brosolo and P. Decleva, Chem. Phys. **159**, 185 (1992).
[3] M. Brosolo, P. Decleva, and A. Lisini, J. Phys. B **25**, 3345 (1992).
[4] M. Brosolo, P. Decleva, and A. Lisini, Comput. Phys. Commun. **71**, 207 (1992).
[5] X. B. Bian, H. P. Liu, and T. Y. Shi, Chin. Phys. Lett. **25**, 2008 (2008).
[6] M. R. Hermann and J. A. Fleck, Jr., Phys. Rev. A **38**, 6000 (1988).
[7] A. D. Bandrauk and H. Shen, Chem. Phys. Lett. **176**, 428 (1991).
[8] G. Avila and T. Carrington, Jr., in *Quantum Dynamic Imaging*, edited by A. D. Bandrauk and M. Ivanov (Springer, New York, 2011), p. 1.
[9] L. Y. Peng and A. F. Starace, J. Chem. Phys. **125**, 154311 (2006).
[10] A. D. Bandrauk, E. Dehghanian, and H. Z. Lu, Chem. Phys. Lett. **419**, 346 (2006).
[11] J. Crank and P. Nicolson, Proc. Cambridge Philos. Soc. **43**, 50 (1947).
[12] Z. G. Sun and W. T. Yang, J. Chem. Phys. **134**, 041101 (2011).
[13] R. Kosloff and H. Tal-Ezer, Chem. Phys. Lett. **127**, 223 (1986).
[14] H. Bachau, E. Cormier, P. Decleva, J. E. Hansen, and F. Martín, Rep. Prog. Phys. **64**, 1815 (2001).
[15] X. B. Bian and A. D. Bandrauk, Phys. Rev. A **83**, 023414 (2011); **83**, 041403(R) (2011).
[16] X. B. Bian, H. X. Qiao, and T. Y. Shi, Chin. Phys. Lett. **23**, 2403 (2006).
[17] C. Froese Fischer and M. Idress, Comput. Phys. **3**, 53 (1989).
[18] L. B. Madsen, L. A. A. Nikolopoulos, T. K. Kjeldsen, and J. Fernández, Phys. Rev. A **76**, 063407 (2007).
[19] Th. Mercouris, Y. Komninos, S. Dionissopoulou, and C. A. Nicolaides, J. Phys. B **30**, 2133 (1997); **29**, L13 (1996).
[20] Th. Mercouris, Y. Komninos, and C. A. Nicolaides, Adv. Quantum Chem. **60**, 333 (2010).
[21] D. R. Bates, U. Öpik, and G. Poots, Proc. Phys. Soc. A **66**, 1113 (1953).
[22] M. M. Madsen and J. M. Peek, Atomic Data and Nuclear Data Tables **2**, 171 (1970).
[23] V. A. Davydkin and L. P. Rapoport, J. Phys. B **7**, 1101 (1974).

[24] S. Kawai and A. D. Bandrauk, Phys. Rev. A **75**, 063402 (2007).
[25] L. I. Ponomarev and L. N. Somov, J. Comput. Phys. **20**, 183 (1976).
[26] H. Bachau, J. Phys. B **35**, 509 (2002).
[27] X. X. Guan, E. B. Secor, K. Bartschat, and B. I. Schneider, Phys. Rev. A **84**, 033420 (2011).
[28] X. X. Guan, K. Bartschat, and B. I. Schneider, Phys. Rev. A **83**, 043403 (2011).
[29] H. Miyagi, T. Morishita, and S. Watanabe, Phys. Rev. A **85**, 022708 (2012).
[30] J. A. Richards and F. P. Larkins, J. Phys. B **19**, 1945 (1986).
[31] J. Colgan, M. S. Pindzola, and F. Robicheaux, Phys. Rev. A **68**, 063413 (2003).
[32] X. B. Bian and A. D. Bandrauk, Phys. Rev. Lett. **105**, 093903 (2010).
[33] G. Lagmago Kamta and A. D. Bandrauk, Phys. Rev. A **75**, 041401 (2007); **76**, 053409 (2007).
[34] G. Lagmago Kamta and A. D. Bandrauk, Phys. Rev. Lett. **94**, 203003 (2005).
[35] J. A. Campos, D. L. Nascimento, D. T. Cavalcante, A. L. A. Fonseca, and A. O. C. Nunes, Int. J. Quantum Chem. **106**, 2587 (2006).
[36] L. J. Zhang, J. M. Feagin, V. Engel, and A. Nakano, Phys. Rev. A **49**, 3457 (1994).
[37] G. W. F. Drake and Z. C. Yan, Chem. Phys. Lett. **229**, 486 (1994).
[38] M. S. Pindzola *et al.*, J. Phys. B **40**, R39 (2007).
[39] C. W. McCurdy and F. Martín, J. Phys. B **37**, 917 (2004).
[40] C. L. Pekeris, Phys. Rev. **126**, 1470 (1962).
[41] S. A. Ndengué, O. Motapon, R. L. Melingui Melono, and A. J. Etindele, J. Phys. B **47**, 015002 (2013).
[42] E. Lorin and A. Bandrauk, Nonlinear Anal. Real World Appl. **12**, 190 (2011).
[43] K. Lopata and N. Govind, J. Chem. Theory Comput. **7**, 1344 (2011).
[44] E. P. Fowe and A. D. Bandrauk, Phys. Rev. A **81**, 023411 (2010).